PAHs and the Universe
C. Joblin and A.G.G.M. Tielens (eds)
EAS Publications Series, **46** *(2011) 453-460*
www.eas.org

SUPERHYDROGENATED PAHS: CATALYTIC FORMATION OF H_2

J.D. Thrower[1], L. Nilsson[1], B. Jørgensen[1], S. Baouche[1], R. Balog[1], A.C. Luntz[1], I. Stensgaard[1], E. Rauls[2] and L. Hornekær[1]

Abstract. The possible role of neutral PAHs as catalysts for H_2 formation in the interstellar medium is investigated by a combined experimental and density function theory study of the superhydrogenation of coronene ($C_{24}H_{12}$). The calculations suggest efficient hydrogenation of both edge and centre sites, along with competing abstraction reactions to form H_2 in a series of catalytic cycles. Scanning tunneling microscopy and thermal desorption measurements have been used to provide direct evidence of the formation of superhydrogenated coronene as a result of exposure to D atoms. Lower limit estimates for the cross-sections of 1.8×10^{-17}, 5.5×10^{-18} and 1.1×10^{-18} cm^2 for the formation of singly, doubly and triply hydrogenated coronene are derived. The results suggest that superhydrogenated PAHs may play an important role in H_2 formation in the ISM.

1 Introduction

The interstellar formation of H_2 remains the subject of intense research effort given the importance of this molecule as a cooling agent and as a key precursor for chemical processes in interstellar dust and molecular clouds. The present consensus is that molecular hydrogen forms on the surface of interstellar dust grains by reactions between hydrogen atoms (Hollenbach & Salpeter 1971). Experiments and theoretical calculations have shown that surface reactions involving physisorbed H atoms are efficient at temperatures below approximately 20 K (Pirronello *et al.* 1997b; Pirronello *et al.* 1997a; Pirronello *et al.* 1999; Katz *et al.* 1999; Manico *et al.* 2001; Roser *et al.* 2002; Hornekær *et al.* 2003; Cuppen & Herbst 2005).

[1] Department of Physics and Astronomy, Aarhus University, 8000 Aarhus C, Denmark
e-mail: liv@phys.au.dk
[2] Department of Theoretical Physics, Faculty of Natural Sciences, University of Paderborn, 33098 Paderborn, Germany

DOI: 10.1051/eas/1146047

In regions with gas temperatures of several hundred kelvin surface reactions involving chemisorbed H atoms have been shown to be efficient (Zecho *et al.* 2002; Cazaux & Tielens 2004; Hornekær *et al.* 2006a, 2006b). However, at intermediate temperatures, no efficient routes for H_2 formation have been identified (Cuppen & Herbst 2005).

A possible alternative route to interstellar H_2 formation is provided by PAH molecules. Observations of spatial correlations between vibrationally excited H_2 and PAHs in photo dissociation regions provide indications of PAHs acting as catalysts for H_2 formation (Habart *et al.* 2003; Habart *et al.* 2004). PAHs in the ISM are thought to exhibit a range of hydrogenation and charge states depending on the environment, especially the UV flux (Le Page *et al.* 2001; Le Page *et al.* 2003; Montillaud *et al.* 2011). At high UV fluxes small PAHs will be dissociated, whilst at intermediate fluxes H loss and ionization dominate, resulting in dehydrogenated and cationic PAHs. Under low UV flux conditions neutral, anionic and superhydrogenated PAHs are likely to be present in the gas phase or frozen out on dust grain surfaces. For example, observations of the 3.4 μm emission aliphatic band in low UV flux regions compare well with laboratory spectra of superhydrogenated neutral PAHs (Bernstein *et al.* 1996). To date, investigations of H_2 formation on PAHs have focussed primarily on cationic states, see, for example, (Le Page *et al.* 1997; Bauschlicher 1998; Betts *et al.* 2006; Le Page *et al.* 2009; Bierbaum 2011). However, formation of H_2 on PAH anions (Bauschlicher & Bakes 2001) and neutral PAHs (Stein & Brown 1991; Bauschlicher 1998; Rauls & Hornekær 2008; Rodriguez *et al.* 2010), as well as on PAH coated grains (Duley & Williams 1993) has also been discussed.

Here we investigate in detail the possible role of neutral PAH molecules and PAH covered dust grains as catalysts for H_2 formation. Density functional theory (DFT) calculations on the hydrogenation of the coronene molecule reveal a relatively small barrier to the addition of a single H atom to coronene. Interestingly, subsequent hydrogenation and abstraction reactions can proceed with little or no barrier, suggesting a catalytic cycle which results in H_2 formation (Rauls & Hornekær 2008). Experimental observations of superhydrogenated coronene formed through exposure to atomic D are also presented. These combined experimental and theoretical results suggest that superhydrogenation of PAHs may provide an important additional route to H_2 formation in intermediate, as well as high temperature environments in the ISM. Similar experimental results for the case of aromatic carbon grain mimics are provided by Mennella (2011).

2 Methods

The DFT calculations were carried out using the plane wave based DACAPO code (Hammer *et al.* 1999; Bahn & Jacobsen 2002) and the PW91 exchange correlation (xc) functional (Perdew *et al.* 1992). Spin polarization was included in all calculations. Potential energy curves were constructed by performing single

https://doi.org/10.1051/eas/1146047 Published online by Cambridge University Press

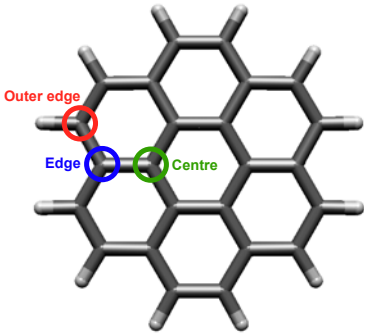

Fig. 1. The possible hydrogenation sites on the coronene molecule. The sites are referred to as outer edge (oe), edge (e) and centre (c).

point calculations with constrained distances between either one H and one C atom, or two H atoms in the case of hydrogenation and abstraction reactions respectively. Barrier heights were obtained by iterative energy calculations within close proximity of the critical geometry. As a result, all barriers can be considered to be upper bounds for the activation energies. See Rauls & Hornekær (2008) for further details.

Scanning tunneling microscopy (STM) and thermal desorption measurements were performed under ultrahigh vacuum (UHV) conditions in two separate chambers. In both chambers, $C_{24}H_{12}$ films were grown by placing the substrate close to an evaporation source in which the $C_{24}H_{12}$ sample was held at 180°C. The coronene films were then exposed to atomic D, which was produced using a hot capillary thermal cracker source of the Jülich type (Tschersich & von Bonin 1998). Temperature programmed desorption (TPD) experiments employed a highly oriented pyrolytic graphite (HOPG) substrate, cleaved prior to mounting in the UHV chamber. TPD spectra were acquired using a quadrupole mass spectrometer (QMS) and a heating ramp of 1 K s^{-1}. A Cu(100) single crystal substrate was used for the STM measurements to exploit the improved imaging conditions provided by the stronger binding between coronene molecules and this substrate.

3 Results

There are three possible sites for the addition of a single H atom to coronene as shown in Figure 1. The most stable product is obtained through addition to a carbon atom in an outer edge site. The additional H atom has a binding energy in excess of 1.4 eV, twice that found for graphite. There is a barrier to addition of 60 meV which is significantly smaller the 200 meV found for H adsorption on the basal plane of graphite (Sha & Jackson 2002). This indicates that hydrogenation of $C_{24}H_{12}$ is likely to occur in cooler environments than for graphite and that the hydrogenated species thus formed will be stable.

https://doi.org/10.1051/eas/1146047 Published online by Cambridge University Press

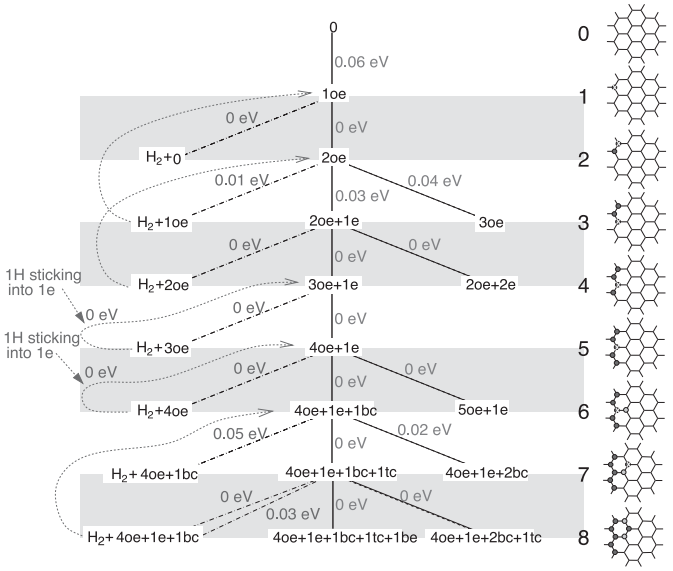

Fig. 2. A summary of the results of the DFT calculations. The central line shows the most favourable addition reactions. The sites involved are indicated. The abstraction reactions and catalytic loops are shown on the left. All energies are the associated reaction barriers. The top and bottom sides of the molecule are labelled t and b respectively. Reproduced by permission of the AAS from Rauls & Hornekær (2008).

Further addition reactions were also considered. The results of these DFT calculations for up to 8 additional H atoms, as well as abstraction reactions from each hydrogenation state, are summarized in Figure 2. Individual potential energy surfaces for these reactions, along a more detailed discussion, can be found elsewhere (Rauls & Hornekær 2008). Addition of a second H atom is most favourable to the outer edge site adjacent to that involved in the first hydrogenation step. This reaction is barrierless and results in a binding energy for the second H atom of 3.2 eV which gives a combined binding energy for the outer edge dimer of *ca.* 4.7 eV. Comparing this value with the H_2 binding energy of 4.5 eV indicates that direct recombination of two bound H atoms to form gas phase H_2 is not energetically favourable. H_2 formation is likely to occur, however, through Eley-Rideal abstraction reactions. Indeed, abstraction by, rather than addition of, the second H atom is also found to be barrierless revealing a competition between these two processes. Similarly, for subsequent incoming H atoms there exist reaction pathways for both addition and abstraction that are thermodynamically viable and have small or even vanishing activation barriers.

Interestingly, not only outer edge and edge sites can be accessed, but a favourable addition to a centre site is also possible with the addition of a sixth H atom.

https://doi.org/10.1051/eas/1146047 Published online by Cambridge University Press

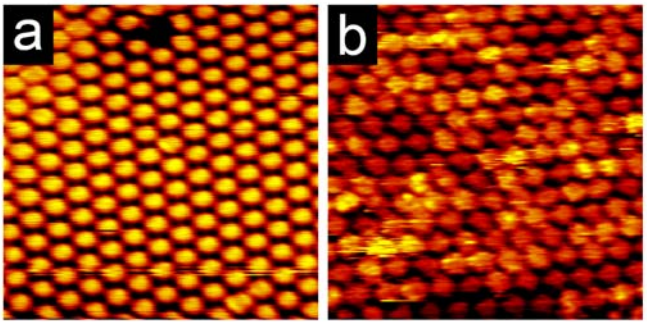

Fig. 3. STM images (150×150 Å^2) of a monolayer of coronene adsorbed on Cu(100) (a) prior to and (b) after exposure to D atoms (4×10^{13} cm^{-2}). The bright protrusions of diameter *ca.* 11.5 Å are identified as individual coronene molecules. Imaging parameters: (a) $V_t = -2460$ mV, $I_t = -0.21$ nA (b) $V_t = -784$ mV, $I_t = -0.17$ nA.

Addition to centre sites occurs such that adjacent H atoms are bound on opposite faces of the molecule. This is consistent with the molecular structure approaching that of the fully hydrogenated coronene molecule, perhydrocoronene ($C_{24}H_{36}$) which exhibits this arrangement of hydrogen atoms. It is clear that the most important step in the hydrogenation process is the addition of the first hydrogen atom. This opens up a series of reaction pathways in which further H atoms may be added with H_2 formation occuring *via* catalytic loops, re-forming lower hydrogenated states. The branching ratios for the competing addition and hydrogenation reactions are not known and will be essential for a full understanding of the efficiency of H_2 formation.

In Figure 3a an STM image of a self-assembled monolayer of $C_{24}H_{12}$ deposited on the clean Cu(100) surface is displayed. An ordered structure of circular protrusions of diameter *ca.* 11.5 Å is observed. These bright protrusions are identified as individual coronene molecules adsorbed flat on the surface. A single vacancy defect is observed in the top part of the image. The coronene covered surface was subsequently exposed to D atoms with a fluence of 4×10^{13} cm^{-2}. An STM image of the surface after exposure is shown in Figure 3b. The image clearly shows variations in imaging intensity between coronene molecules, as well as within individual coronene molecules. These variations are attributed to the formation of hydrogenated coronene. The range of different intensity variations in the image suggests the presence of coronene molecules with differing degrees of hydrogenation. Comparison between STM images and theoretical calculations should make it possible to determine the number and position of deuterium atoms added to individual coronene molecules in the near future.

Thermal desorption measurements have also been conducted using a layer of $C_{24}H_{12}$ grown on the HOPG substrate and subsequently exposed to D atoms with a fluence of 9×10^{15} cm^{-2}. The substrate was then heated linearly and the desorbing

https://doi.org/10.1051/eas/1146047 Published online by Cambridge University Press

Table 1. Contributions to the desorption signal from the different hydrogenation states along with estimated lower limits for the associated addition reaction cross-sections.

m/z	% of desorption signal	cross-section / cm^2
300	77	—
302	16	1.8×10^{-17}
304	5	5.5×10^{-18}
306	1	1.1×10^{-18}

species detected. Desorption signals (not shown) for $m/z = 300$, 302, 304 and 306 corresponding to coronene and singly, doubly and triply hydrogenated (with D) products were observed. Table 1 shows the relative contributions to the total desorption signal for the individual hydrogenation states observed. The estimated reaction cross-sections are based on the following assumptions: only contribution from one coronene layer (correct within a factor of 2–3), no saturation effects, detection of all hydrogenated species. For the doubly and triply hydrogenated coronene the values derived are the effective overall cross-sections obtained using the total initial coronene coverage. Since the electron impact ionization employed in the QMS is likely to lead to fragmentation and dehydrogenation, the calculated cross-sections are only lower limits. The cross-sections thus derived are larger than those found previously for the irradiation of carbon grain mimics (*ca.* 2×10^{-18} cm^2) with H atoms at temperatures of 80–300 K (Mennella *et al.* 2002; Mennella 2006). This is consistent with the use of significantly higher D atom temperatures in the present study. At higher D atom fluences, even higher degrees of superhydrogenation of coronene are observed.

4 Conclusions

DFT calculations indicate the presence of energetically favourable pathways to H_2 formation through catalytic cycles of hydrogenation and abstraction. The barrier to addition of the first H atom is of the order of 60 meV and small or vanishing barriers are found for all subsequent reactions. The hydrogenation of coronene has been observed directly using STM through the appearance of sub-molecular structure following exposure to D atoms. There is evidence for the presence of several different hydrogenated species, although comparison with theory will be required to determine the degree of hydrogenation and the sites involved. Thermal desorption measurements show that very high levels of superhydrogenation can be attained. Hence, both theoretical calculations and experimental results indicate that PAHs might well play a role as catalysts for H_2 formation in intermediate and high temperature environments.

https://doi.org/10.1051/eas/1146047 Published online by Cambridge University Press

The authors gratefully acknowledge financial support from the European Research Council under ERC starting grant HPAH, No. 208344. The research leading to these results has received funding from the European Community's Seventh Framework Programme under grant agreement No. 238258.

References

Bahn, S.R., & Jacobsen, K.W., 2002, Comput. Sci., 4, 56

Bauschlicher, C.W., 1998, ApJ, 509, L125

Bauschlicher, C.W., & Bakes, E.L.O., 2001, Chem. Phys., 274, 11

Bernstein, M.P., Sandford, S.A., & Allamandola, L.J., 1996, ApJ, 472, L127

Betts, N.B., Stepanovic, M., Snow, T.P., & Bierbaum, V.M., 2006, ApJ, 651, L129

Bierbaum, V.M., 2011, this volume

Cazaux, S., & Tielens, A.G.G.M., 2004, ApJ, 604, 222

Cuppen, H.M., & Herbst, E., 2005, MNRAS, 361, 565

Duley, W.W., & Williams, D.A., 1993, MNRAS, 260, 37

Habart, E., Boulanger, F., Verstraete, L., *et al.*, 2003, A&A, 397, 623

Habart, E., Boulanger, F., Verstraete, L., Walmsley, C.M., & des Forets, G.P., 2004, A&A, 414, 531

Hammer, B., Hansen, L.B., & Norskov, J.K., 1999, Phys. Rev. B, 59, 7413

Hollenbach, D., & Salpeter, E.E., 1971, ApJ, 163, 155

Hornekær, L., Baurichter, A., Petrunin, V.V., Field, D., & Luntz, A.C., 2003, Science, 302, 1943

Hornekær, L., Rauls, E., Xu, W., *et al.*, 2006a, Phys. Rev. Lett., 97, 186102

Hornekær, L., Sljivancanin, Z., Xu, W., *et al.*, 2006b, Phys. Rev. Lett., 96, 156104

Katz, N., Furman, I., Biham, O., Pirronello, V., & Vidali, G., 1999, ApJ, 522, 305

Le Page, V., Snow, T.P., & Bierbaum, V.M., 2001, ApJS, 132, 233

Le Page, V., Snow, T.P., & Bierbaum, V.M., 2003, ApJ, 584, 316

Le Page, V., Snow, T.P., & Bierbaum, V.M., 2009, ApJ, 704, 274

LePage, V., Keheyan, Y., Bierbaum, V.M., & Snow, T.P., 1997, J. Am. Chem. Soc., 119, 8373

Manico, G., Raguni, G., Pirronello, V., Roser, J.E., & Vidali, G., 2001, ApJ, 548, L253

Mennella, V., 2006, ApJ, 647, L49

Mennella, V., Brucato, J.R., Colangeli, L., & Palumbo, P., 2002, ApJ, 569, 531

Mennella, V., 2011, this volume

Montillaud, J., Joblin, C., Toublanc, D., *et al.*, 2011, this volume

Perdew, J.P., Chevary, J.A., Vosko, S.H., *et al.*, 1992, Phys. Rev. B, 46, 6671

Pirronello, V., Biham, O., Liu, C., Shen, L.O., & Vidali, G., 1997a, ApJ, 483, L131

Pirronello, V., Liu, C., Roser, J.E., & Vidali, G., 1999, A&A, 344, 681

Pirronello, V., Liu, C., Shen, L., & Vidali, G., 1997b, ApJ, 475, L69

Rauls, E., & Hornekær, L., 2008, ApJ, 679, 531

Rodriguez, L.S., Ruette, F., Sanchez, M., & Mendoza, C., 2010, J. Mol. Catal. A, 316, 16

Roser, J.E., Manico, G., Pirronello, V., & Vidali, G., 2002, ApJ, 581, 276

Sha, X.W., & Jackson, B., 2002, Surf. Sci., 496, 318

Stein, S.E., & Brown, R.L., 1991, J. Am. Chem. Soc., 113, 787

Tschersich, K.G., & von Bonin, V., 1998, J. Appl. Phys., 84, 4065

Zecho, T., Güttler, A., Sha, X., Jackson, B., & Küppers, J., 2002, J. Chem. Phys., 117, 8486

https://doi.org/10.1051/eas/1146047 Published online by Cambridge University Press